Available online at www.sciencedirect.com
ScienceDirect
Journal of the European Ceramic Society 28 (2008) 3119–3124
www.elsevier.com/locate/jeurceramsoc

Phase relations and electrical properties in the pseudo-ternary La_2O_3–TiO_2–Mn_2O_3 system in air

Srečo Davor Škapin *, Špela Kunej, Danilo Suvorov

"Jožef Stefan" Institute, Jamova 39, 1000 Ljubljana, Slovenia

Received 26 February 2008; received in revised form 16 May 2008; accepted 27 May 2008
Available online 7 July 2008

Abstract

Scanning electron microscopy (SEM), electron-probe microanalysis, energy- and wavelength-dispersive X-ray analysis and X-ray powder diffraction were used to investigate the subsolidus phase relations in the pseudo-ternary La_2O_3–TiO_2–Mn_2O_3 system in air (oxygen partial pressure $p_{O_2} = 0.21$ atm) at 1275 °C. The addition of Mn_2O_3 to the starting La_2O_3:3TiO_2 mixture led to the formation of a La-deficient perovskite $La_{2/3}TiO_3$ compound. The oxides form two new compounds with the proposed compositions: (i) $La_{1.7}Ti_{13.0}Mn_{6.3}O_{38-x}$, with a davidite-like crystal structure, and (ii) $La_{49}Ti_{18}Mn_{13}O_{129}$. There were also several solid solutions existing over a wide range of concentrations.

Keywords: Phase equilibria; Microstructure-final; Dielectric properties; Perovskites; $La_{2/3}TiO_3$

1. Introduction

Compounds in the R_2O_3–TiO_2 (R: La, Nd) system show a good combination of dielectric properties, which makes them potential candidates for various components in electronic circuits.[1–4] Their properties can be improved even further by the addition of small amounts of some oxides (or compounds) that promote the formation of a perovskite-like $R_{2/3}TiO_3$ compound in these systems.[5–7]

It is known that the $R_{2/3}TiO_3$ compound is not stable in its pure form due to the large number of vacant A sites in the crystal structure;[9] however, as little as 4 mol% of $LaAlO_3$ can fully stabilize the $La_{2/3}TiO_3$ compound.[5,8] Ceramics based on the $La_{2/3}TiO_3$–$LaAlO_3$ system were reported to possess interesting microwave dielectric properties with a high level of tunebility.[6]

In terms of chemical properties manganese closely resembles aluminum. The similarity of the ionic radii of the two elements (0.53 Å for Al^{3+} and 0.645 Å for Mn^{3+} in an octahedral coordination)[10] could permit the formation of isostructural compounds and a solid solution with similar dielectric properties. The oxides La_2O_3 and TiO_2 are stable up to high temperatures, >1300 °C; however, Mn_2O_3 transforms to tetragonal Mn_3O_4 during heating in air at ≈970 °C, and this phase further transforms into cubic Mn_3O_4 at 1170 °C, which is then stable up to ≈1560 °C.[11,12]

Two compounds, $LaMnO_{3\pm\delta}$ and $La_2MnO_{4+\delta}$, exist in the La_2O_3–Mn_2O_3 system.[13] Only the perovskite-type $LaMnO_{3+\delta}$ compound is stable in air; however, the $La_2MnO_{4+\delta}$ compound forms in atmospheres with a low oxygen pressure at temperatures higher than 1300 °C.[13] The phase diagram of the system in air was constructed by van Roosmalen *et al.*[14] The $LaMnO_3$ compound has the narrow solid-solubility range of La_2O_3 and Mn_2O_3, which is ≈2 mol% of each oxide, at ≈1300 °C.[13,14]

When sintering $LaMnO_3$ at high temperatures some of the Mn^{3+} oxidizes into Mn^{4+}, resulting in the formation of defects on the cation sites in equal amounts.[15] Thus, the real composition is $La_{1-\varepsilon}Mn_{1-\varepsilon}O_3$, although the expression $LaMnO_{3\pm\delta}$ is usually used in the literature. This perovskite structure allows a large deviation from stoichiometry, with the δ value depending on the sintering temperature and the oxygen partial pressure.

Phase equilibria in the Mn–Ti–O system in air were studied by Chufarov *et al.*[16] It is evident from their phase diagram that the Mn_2O_3 and TiO_2 form a $Mn_xTi_{3-x}O_4$ solid solution at 1300 °C with a spinel crystal structure, where x varies from 3 to 2.48, and an ilmenite-like $MnTiO_3$ compound.

Phase relations in the La_2O_3–TiO_2 binary system are well described.[17,18] The stable compounds are $La_4Ti_9O_{24}$, $La_2Ti_2O_7$, $La_4Ti_3O_{12}$ and La_2TiO_5.

* Corresponding author. Tel.: +386 1 477 37 08; fax: +386 1 477 38 75.
E-mail address: sreco.skapin@ijs.si (S.D. Škapin).

0955-2219/$ – see front matter © 2008 Elsevier Ltd. All rights reserved.
doi:10.1016/j.jeurceramsoc.2008.05.022

In this study we have established the subsolidus phase equilibria in the pseudo-ternary La_2O_3–TiO_2–Mn_2O_3 system at 1275 °C, where new ternary compounds and solid solutions were identified. The proposed phase diagram represents a section through the system for the normal oxygen pressure in air at 1 atm, with the compositions being expressed in terms of the oxide components that are stable at room temperature.

2. Experimental procedure

The samples were prepared by a conventional solid-state reaction method from individual oxide powders: La_2O_3 (Johnson Matthey 99.9%), TiO_2 (Johnson Matthey 99.8%) and Mn_2O_3 (Johnson Matthey 98%). The samples were first weighed out in the different ratios. Due to the strong tendency of La_2O_3 to form a hydroxide and a carbonate with the moisture and the CO_2 in the air the oxide was routinely checked prior to weighing with an ignition-loss measurement at 1300 °C. The samples were fired at least three times at 1275 °C for approximately 5 h, with intermittent crushing, mixing and homogenization in order to achieve equilibrium. The phases in the prepared samples were identified using X-ray powder diffractometry (XRD) (Model PW 1710, Netherlands Philips). The crystal-structure parameters for the davidite-like compound were calculated using the program TOPAS 2R. Polished cross-sections of the samples were examined by scanning electron microscopy (SEM) (Jeol JXA 840A, Japan) and a quantitative analysis of the phases present was performed with wavelength-dispersive spectroscopy (WDS) and energy-dispersive spectroscopy (EDS) using TRACOR software (Tracor Northern, Model NORAN Series II, USA). The WDS analysis measurements were carried out on a PET crystal for the spectral lines LaLα1, TiKα1, MnKα1 at 20 kV, a 15-nA electron beam current, and a 40° take-off angle. The ZAF matrix-correction procedure was then used to quantify each element. The standards used were $La_2Ti_2O_7$ and Mn_3O_4. The capacitance and dielectric losses were measured at 1 MHz with a Hewlett Packard 4192A LF impedance analyzer in the temperature range from −20 to 120 °C using Heraeus Voetsch chamber.

3. Results and discussion

Based on the firing experiments in air we constructed a phase diagram of the pseudo-ternary La_2O_3–TiO_2–Mn_2O_3 system in air at 1275 °C (Fig. 1).

In this system the phase relations are shown as a projection onto the La_2O_3–TiO_2–Mn_2O_3 system for the sake of simplicity. Thus, the systems TiO_2–Mn_2O_3 and La_2O_3–Mn_2O_3 are presented as dashed lines.

In the pseudo-ternary system we identified a stabilized $La_{2/3}TiO_3$ compound, two new ternary compounds and several solid solutions.

3.1. Ternary compounds in the La_2O_3–TiO_2–Mn_2O_3 system

(1) The stabilization of an unstable perovskite $La_{2/3}TiO_3$ compound with the addition of $LaMnO_3$ can be described by the following reaction:

$$(1-x)La_{2/3}TiO_3 + xLaMnO_3 \rightarrow La_{(2+x)/3}Ti_{1-x}Mn_xO_3, \quad (1)$$

where we assumed, based on ionic size, that the Mn enters into the B sites and the La into the A sites in the perovskite structure. Thus, for $x = 0$, two phases were identified: $La_4Ti_9O_{24}$ and $La_2Ti_2O_7$ (Fig. 2, pattern a). Increasing the x value ($x = 0.01$) resulted in the appearance of a third phase: stabilized $La_{2/3}TiO_3$ (Eq. (1), Fig. 2, pattern b). The amount of this phase increased with an increasing x value. Fig. 3a shows a microstructure of the sample with $x = 0.03$, containing the $La_{2/3}TiO_3$, $La_2Ti_2O_7$ and $La_4Ti_9O_{24}$ phases (Fig. 2, pattern c). The sample with the composition $x = 0.06$ was composed mainly of $La_{2/3}TiO_3$, with a small amount of $La_2Ti_2O_7$ phase (Fig. 2, pattern d). However, the amount of $La_{2/3}TiO_3$ phase could be decreased by further increasing the x values. Detailed EDS analyses of the $La_{2/3}TiO_3$ phase in different samples showed that it was stable in a rather narrow concentration range, $0.04 \leq x \leq 0.06$.

(2) In the sample with $x = 0.10$ a new phase was identified by using SEM and XRD, and the $La_4Ti_9O_{24}$ phase disappeared (Fig. 2, pattern e).

The proposed composition of the new phase, based on WDS analyses, was $La_{1.7}Ti_{13.0}Mn_{6.3}O_{38-x}$ (abbreviated as LTM1). From its XRD pattern it could be concluded that the compound is isostructural with the $La_2Ti_{10.27}Ga_{9.63}O_{38}$[19] compound formed in the La_2O_3–TiO_2–Ga_2O_3 system, which exhibits a davidite-like crystal structure.[20] It can be expected that a limited part of the Mn^{3+} is reduced to Mn^{2+}, like with the isoctructural compound $LaFe_4Ti_6O_{19}$.[21]

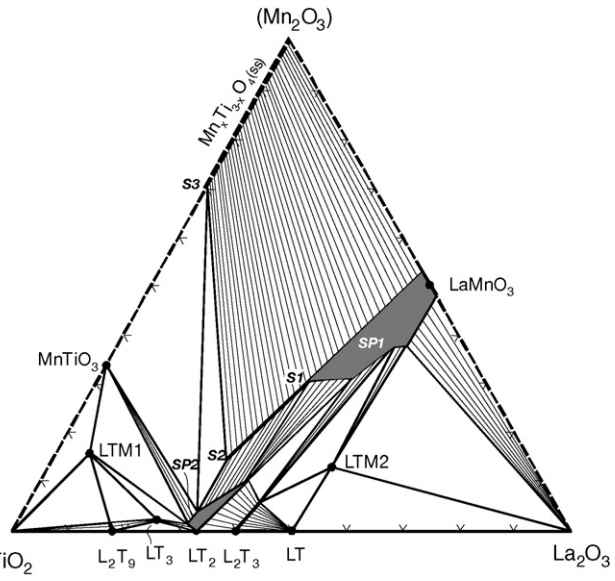

Fig. 1. Pseudo-ternary subsolidus phase diagram of the La_2O_3–TiO_2–Mn_2O_3 system in air, equilibrated at 1275 °C (L_2T_9: $La_4Ti_9O_{24}$, LT_3: $La_{2/3}TiO_3$, LT_2: $La_2Ti_2O_7$, L_2T_3: $La_4Ti_3O_{12}$ and LT: La_2TiO_5).

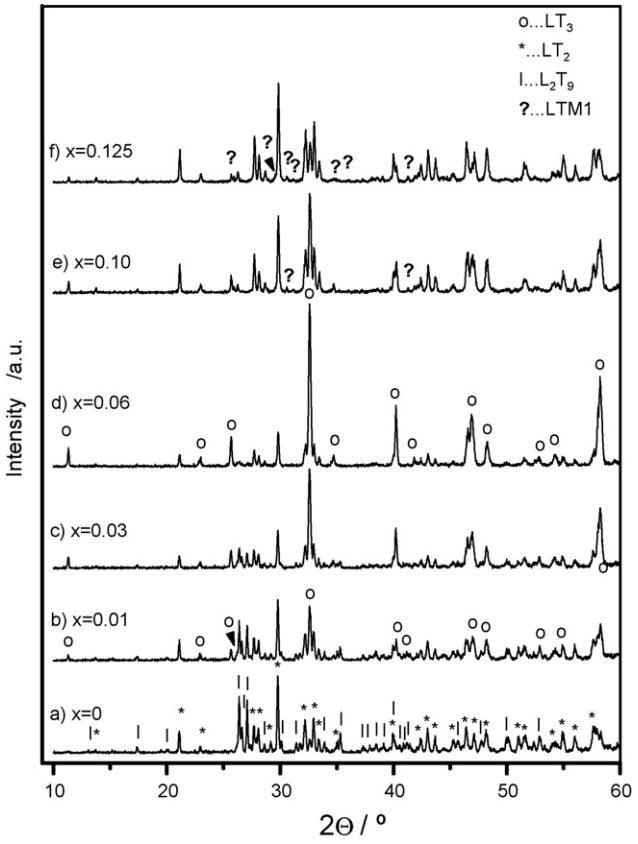

Fig. 2. XRD patterns of the samples prepared according to the scheme $(1-x)La_{2/3}TiO_3 - xLaMnO_3$ ($x = 0$, 0.01, 0.03, 0.06, 0.10 and 0.125). The stabilized $La_{2/3}TiO_3$ phase already appears in the sample with the composition $x = 0.01$, and at the composition $x = 0.06$ the sample contains a perovskite phase and a small amount of the $La_2Ti_2O_7$ phase. At the composition $x = 0.10$ the weak peaks of the LTM1 phase appear and at $x = 0.125$ these peaks became more intense.

The compound LTM1 crystallizes in a rhombohedral structure (space group R-3) with the refined unit-cell parameters $a = 9.288(1)$ Å, $\alpha = 68.48(1)^\circ$ and $V = 667.92(5)$ Å^3.

(3) The composition of the second new compound was determined by WDS and XRD analyses of many samples that were prepared in the La_2O_3-rich part of the system and was 50 mol% La_2O_3, 36.7 mol%TiO_2 and 13.3 mol% Mn_2O_3, corresponding to the formula $La_{49}Ti_{18}Mn_{13}O_{129}$ (labeled as LTM2). This composition lies on the $LaMnO_3$–La_2TiO_5 tie line.

A detailed crystal-structure determination of both compounds with Rietweld refinements is the subject of a further investigation.

3.2. Solid solution in the TiO_2–Mn_2O_3 system

Experimental results confirmed the formation of the $Mn_xTi_{3-x}O_4$ solid solution in the concentration range $3 \leq x \leq \approx 2.5$ (point *S3* in Fig. 1), which agrees well with the literature data.[16]

3.3. Solid solution based on $LaMnO_3$

According to our XRD results ≈2 mol% La_2O_3 and ≈2 mol% Mn_2O_3 can be dissolved in the $LaMnO_3$, which agrees well with the reported data.[14]

The perovskites $LaMnO_3$ and $La_{2/3}TiO_3$ form a solid solution over a wide concentration range. The incorporation of La_2O_3 and TiO_2 in the molar ratio 1:3 (corresponding to the $La_{2/3}TiO_3$ compound) in $LaMnO_3$ can be described with the following simplified expression:

$$(1-x)LaMnO_3 + xLa_{2/3}TiO_3 \rightarrow La_{1-x/3}Mn_{1-x}Ti_xO_3, \quad (2)$$

where x varies from 0 to 0.663 [$LaMnO_3$(ss)], corresponding to the formula $La_{0.779}Mn_{0.337}Ti_{0.663}O_3$. This saturated $LaMnO_3$(ss) contains up to ≈54 mol% TiO_2 (point *S2* in Fig. 1). The actual composition of the $LaMnO_3$(ss) may have deviated slightly from the proposed one because the La:Mn ratio in the starting $LaMnO_3$ was not 1:1, but 0.96:1.04.

The $LaMnO_3$ is connected with the tie lines to the other lanthanum titanates: $La_2Ti_2O_7$, $La_4Ti_3O_{12}$ and La_2TiO_5. The tie lines are pointed at $LaMnO_3$ with 2 mol% dissolved La_2O_3. This composition of the $LaMnO_3$ with La:Mn = 1.04:0.96 dissolves:

(1) $La_2Ti_2O_7$, up to ≈24.6 mol% TiO_2.
(2) $La_4Ti_3O_{12}$, up to ≈12.9 mol% TiO_2.
(3) La_2TiO_5, up to ≈10.7 mol% TiO_2.

The solid solutions $LaMnO_3$–$La_{2/3}TiO_3$ on the one side and $LaMnO_3$–$La_2Ti_2O_7$ and $LaMnO_3$–$La_4Ti_3O_{12}$ on the other, circumscribe a single-phase area based on $LaMnO_3$, labeled as *SP1*, which is marked with a grey color in the phase diagram in Fig. 1.

3.4. Solid solutions based on the lanthanum titanates

The lanthanum titanates ($La_4Ti_9O_{24}$, $La_2Ti_2O_7$ and $La_4Ti_3O_{12}$) dissolve Mn_2O_3 together with La_2O_3 and/or TiO_2:

(1) $La_4Ti_9O_{24}$ dissolves the LTM1 compound up to ≈2 mol% Mn_2O_3.
(2) $La_2Ti_2O_7$ dissolves—the LTM1 compound up to ≈2 mol% Mn_2O_3,
   - $MnTiO_3$ up to ≈3 mol% Mn_2O_3,
   - the $Mn_xTi_{3-x}O_4$ solid solution with the TiO_2-saturated composition (*S3*, $x \approx 2.5$), up to ≈3 mol% Mn_2O_3,
   - the $LaMnO_3$ (La:Mn = 1.04:0.96) up to ≈10 mol% Mn_2O_3.

Thus, the $La_2Ti_2O_7$ forms a single-phase area, labeled as *SP2* and marked with a grey color in the phase diagram (Fig. 1).

(3) $La_4Ti_3O_{12}$ dissolves $LaMnO_3$ (with La:Mn = 1.04:0.96) up to ≈6 mol% Mn_2O_3. The solid solubility of the $LaMnO_3$ in the La_2TiO_5 was not confirmed.

3.5. Description of the phase relations

A large two-phase field predominates in the Mn_2O_3-rich corner of the system. The phases in equilibrium at 1275 °C are the spinel-like $Mn_xTi_{3-x}O_4$ solid solution, where the titania content varies up to ≈30 mol% TiO_2 (point *S3*) and $LaMnO_3$(ss) along the whole region of $La_{2/3}TiO_3$ solid solubility (up to point *S2*). The co-nodes that connect the equilibrium compositions from both phases were confirmed by WDS analyses of the phases in the microstructures of several samples.

The locations of the co-nodes in the two-phase area, where the phases are $La_2Ti_2O_7$(ss) and $LaMnO_3$(ss) in the range from *S1* to *S2*, were also determined with WDS analyses because the samples prepared in this area were successfully sintered and detailed microstructural analyses were performed.

On the basis of the XRD and the microanalyses (EDS and WDS) of the samples prepared in this system in air, the following tie lines were confirmed:

Table 1
Dielectric properties of the ceramics based on $(1-x)La_{2/3}TiO_3 - xLaMnO_3$, sintered at 1275 °C

x in $(1-x)LT_3 - xLM$	$\varepsilon_{20\,°C}$	$\tan\delta \times 10^4$	τ_k [ppm/K]
0.0	47	<1	−89
0.02	52.6	9	−118
0.025	55.6	13	−110
0.03	57.4	27	−70
0.035	61.1	44	−42
0.04	62.8	50	−17
0.045	66.8	48	−26
0.05	66.2	55	−53
0.055	73.0	30	−72
0.06	73.7	37	−53
0.07	73.5	26	−58
0.10	60.0	30	40

The measurements were performed at a frequency of 1 MHz and at room temperature. LT_3: $La_{2/3}TiO_3$, LM: $LaMnO_3$.

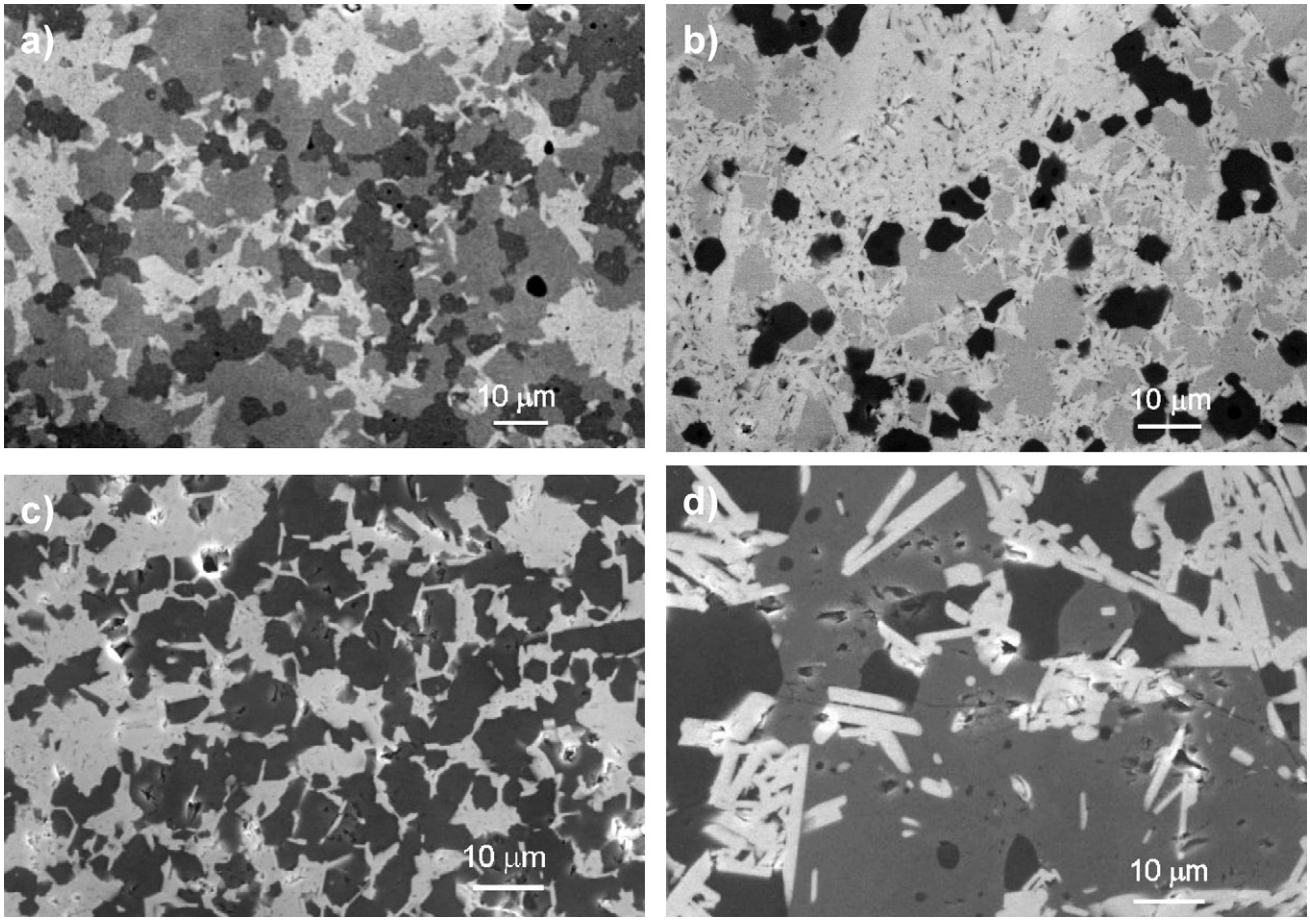

Fig. 3. SEM micrographs of the polished cross-sections of selected samples prepared in the system La_2O_3–TiO_2–Mn_2O_3:
(a) The sample with the composition $0.97La_{2/3}TiO_3$–$0.03LaMnO_3$ contains a bright phase, $La_2Ti_2O_7$(ss); a grey phase, $La_{2/3}TiO_3$; and a dark phase, $La_4Ti_9O_{24}$.
(b) The sample with the starting composition 25 mol% La_2O_3:71 mol% TiO_2:4 mol% Mn_2O_3, is composed of a bright phase, $La_2Ti_2O_7$(ss); a grey phase, $La_{2/3}TiO_3$; and a dark phase, LTM1.
(c) The sample with the starting composition 12 mol% La_2O_3:65 mol% TiO_2:23 mol% Mn_2O_3, is composed of a bright phase, $La_2Ti_2O_7$(ss); and a dark phase, LTM1.
(d) The sample with the starting composition 15 mol% La_2O_3:55 mol% TiO_2:30 mol% Mn_2O_3, is composed of a bright phase, $La_2Ti_2O_7$(ss); a grey phase, $MnTiO_3$; and a dark phase, $Mn_xTi_{3-x}O_4$(ss).

- The LTM1 compound is in equilibrium with TiO_2, $MnTiO_3$, $La_4Ti_9O_{24}$(ss), $La_{2/3}TiO_3$ and $La_2Ti_2O_7$(ss). The microstructure of the sample containing the LTM1 phase coexisting with $La_{2/3}TiO_3$ and $La_2Ti_2O_7$ is presented in Fig. 3b,
- the stabilized $La_{2/3}TiO_3$ compound is in equilibrium with $La_4Ti_9O_{24}$, LTM1 and $La_2Ti_2O_7$,
- the $La_2Ti_2O_7$ is connected with tie lines to $La_{2/3}TiO_3$, LTM1, $MnTiO_3$, $Mn_xTi_{3-x}O_4$(ss) and $LaMnO_3$(ss). Fig. 3c shows the two-phase microstructure of the sample that is composed of $La_2Ti_2O_{7(ss)}$ and $MnTiO_3$, and Fig. 3d shows the three-phase microstructure of the sample containing $La_2Ti_2O_7$(ss), $MnTiO_3$ and $Mn_xTi_{3-x}O_4$(ss),
- the $La_4Ti_3O_{12}$ coexists with $La_2Ti_2O_7$(ss), $LaMnO_3$(ss), La_2TiO_5 and LTM2,
- the LTM2 compound is in equilibrium with $LaMnO_3$(ss), $La_4Ti_3O_{12}$(ss), La_2TiO_5 and La_2O_3.

3.6. Dielectric properties

The dielectric properties of the $(1-x)La_{2/3}TiO_3$–$xLaMnO_3$ compositions in the composition range $0.0 \le x \le 0.1$ are shown in Table 1 (measured at 1 MHz). The permittivity (ε) of the analyzed ceramics increases with the increasing amount of the stabilized $La_{2/3}TiO_3$ phase in the samples; it reaches a maximum value $\varepsilon \approx 73$ at $x = 0.06$, after which it decreases for larger $LaMnO_3$ additions.

The dielectric losses ($\tan\delta$) of the samples with the composition $0.02 \le x \le 0.10$ increase up to the composition $x = 0.05$ and then decrease with a further increase in the $LaMnO_3$ additions. The dielectric losses are rather high, compared to those in the system La_2O_3–TiO_2–Ga_2O_3.[19] It seems that such behaviour is associated with the amount of Mn-stabilized $La_{2/3}TiO_3$ phase in the samples. In this phase with the proposed formula $La_{(2+x)/3}Ti_{1-x}Mn_xO_3$ (Eq. (1)) a limited part of the manganese in the B sites of the perovskite structure may be ionized to Mn^{4+} ions, resulting in the formation of free electrons. The ionization can be described by the following expression (Kroeger–Vink notation is used):

$$(Mn_{Ti})' \rightarrow (Mn_{Ti})^x + n' \quad (3)$$

Such an ionization, where charge carriers are generated, may explain the large dielectric losses. The same oxidation process of Mn^{3+} into Mn^{4+} also takes place during the sintering, like with $LaMnO_{3\pm\delta}$.[15]

The temperature coefficient of the dielectric constant (τ_k) is given for the temperature region from 20 to 80 °C. In this range the τ_k shows a linear temperature dependence.

4. Conclusions

The subsolidus phase relations in the pseudo-ternary La_2O_3–TiO_2–Mn_2O_3 system in air at 1275 °C were determined. The addition of a small amount of $LaMnO_3$ to La_2O_3:3TiO_2 resulted in the stabilization of a perovskite $La_{2/3}TiO_3$ compound with the formula $La_{(2+x)/3}Ti_{1-x}Mn_xO_3$. This compound is stable within a narrow concentration range $0.04 \le x \le 0.06$. Additionally, two new compounds were identified in the system: (i) $La_{1.7}Ti_{13.0}Mn_{6.3}O_{38-x}$, with a davidite-like crystal structure, and (ii) $La_{49}Ti_{18}Mn_{13}O_{129}$. $La_{2/3}TiO_3$, $La_2Ti_2O_7$, $La_4Ti_3O_{12}$ and $LaTiO_5$ dissolve in $LaMnO_3$ and form a single-phase area based on $LaMnO_3$(ss) in an extended concentration range. Similarly, $La_2Ti_2O_7$ dissolves $LaMnO_3$ and LTM1, resulting in a single-phase area based on $La_2Ti_2O_7$(ss). Some limited solid solubility of $LaMnO_3$ in $La_4Ti_3O_{12}$ and LTM1 in $La_4Ti_9O_{24}$ was also confirmed in the system. The dielectric measurements of the compositions containing the stabilized $La_{2/3}TiO_3$ phase revealed that the properties depended on the amount of $La_{2/3}TiO_3$ in the samples. The highest room-temperature permittivity ($\varepsilon = 73.7$) was exhibited by the nearly single-phase $La_{2/3}TiO_3$-based ceramic, with a temperature coefficient $\tau_f = -55$ ppm/°C and a dielectric loss $\tan\delta = 37 \times 10^{-4}$, at 1 MHz.

Acknowledgement

This work was supported by the Slovenian Research Agency (Grant P2-0091-0106).

References

1. Marzulo, S. and Bunting, E. N., Dielectric properties of titania or tin oxide containing varying proportions of rare-earth oxides. *J. Am. Ceram. Soc.*, 1958, **41**, 40–41.
2. Yokoyama, M., Ota, T., Yamai, I. and Takahashi, J., Flux growth of perovskite-type $La_{2/3}TiO_{3-x}$ crystals. *J. Cryst. Growth*, 1989, **96**, 490–496.
3. Takahashi, J., Kageyama, K. and Hayashi, T., Dielectric properties of double-oxide ceramics in the system Ln_2O_3–TiO_2 (Ln = La, Nd and Sm). *Jpn. J. Appl. Phys.*, 1991, **30**(9B), 2354–2358.
4. Fuierer, P. A. and Newnham, R. E., $La_2Ti_2O_7$ ceramics. *J. Am. Ceram. Soc.*, 1991, **74**(11), 2876–2881.
5. Škapin, S. D., Kolar, D. and Suvorov, D., X–ray diffraction and microstructural investigation of the Al_2O_3–La_2O_3–TiO_2 system. *J. Am. Ceram. Soc.*, 1993, **76**(9), 2359–2362.
6. Suvorov, D., Valant, M., Škapin, S. D. and Kolar, D., Microwave dielectric properties of ceramics with compositions along the $La_{2/3}TiO_{3(STAB)}$–$LaAlO_3$ tie line. *J. Mater. Sci.*, 1997, **33**, 85–89.
7. Škapin, S. D. and Suvorov, D., High-temperature phase relations in multicomponent oxide ceramics that are important for advanced electronic ceramics development, selected papers from YUCOMAT IV. 4th Yugoslav Materials Research Society Conference, 2001. *Mater. Sci. Forum*, 2003, **413**, 115–120.
8. Negas, T., Yeager, G., Bell, S. and Amren, R., Chemistry and properties of temperature compensated microwave dielectrics. *Chem. Electron. Ceram. Mater.*, 1991, 21–37 (NIST Special Publication 804).
9. Abe, M. and Uchino, K., X-ray study of the deficient perovskite $La_{2/3}TiO_3$. *Mater. Res. Bull.*, 1974, **9**, 147–156.
10. Shannon, D., Revised effective ionic radii and systematic studies of interatomic distances in halides and chalcogenides. *Acta Cryst.*, 1976, **A32**, 751–767.
11. Metselaar, R., Van Tol, R. E. J. and Piercy, P., The electrical conductivity and thermoelectric power of Mn_3O_4 at high temperatures. *J. Solid State Chem.*, 1981, **38**, 335–341.
12. Dorris, S. E. and Mason, T. O., Electrical properties and cation valencies in Mn_3O_4. *J. Am. Ceram. Soc.*, 1988, **71**(5), 379–385.
13. Cherepanov, V. A., Barkhatova, L. Yu. and Voronin, V. I., Phase equilibria in the La-Sr-Mn-O system. *J. Solid State Chem.*, 1997, **134**, 38–44.
14. van Roosmalen, J. A. M., van Vlaanderen, P., Cordfunke, E. H. P., IJdo, W. L. and IJdo, D. J. W., Phases in the perovskite-type $LaMnO_{3+\delta}$ solid

solution and the La_2O_3–Mn_2O_3 phase diagram. *J. Solid State Chem.*, 1995, **114**, 516–523.
15. van Roosmalen, J. A. M., Cordfunke, E. H. P., Helmholdt, R. B. and Zandbergen, H. W., The defect chemistry of $LaMnO_{3\pm\delta}$; 2. Structural aspects of $LaMnO_{3+\delta}$. *J. Solid State Chem.*, 1995, **110**, 100–105.
16. Chufarov, G. I., Yankin, A. M., DeminYu., V. P., Golikov, V. and Balakirev, V. F., Fazovnie Diagrammi Sistemi Mn-Ti-O na Vozduhe. *Zh. Fiz. Khim.*, 1986, **60**(4), 863–866.
17. MacChesney, J. B. and Sauer, H. A., The system La_2O_3–TiO_2; phase equilibria and electrical properties. *J. Am. Ceram. Soc.*, 1962, **45**(9),416–422.
18. Škapin, S. D., Kolar, D. and Suvorov, D., Phase stability and equilibria in the La_2O_3–TiO_2 system. *J. Eur. Ceram. Soc.*, 2000, **20**, 1179–1185.
19. Kolar, D., Škapin, S. D., Suvorov, D. and Valant, M., Phase equilibria and dielectric properties in the La_2O_3–Ga_2O_3–TiO_2 system. In *Proceedings of the Ninth International Conference on High Temperature Materials Chemistry, vol. IX*, ed. SPEAR and E. Karl. The Electrochemical Society, Pennington, 1997, pp. 109–115 (Proceedings, vol. 97-39).
20. Meden, A., Kolar, D. and Škapin, S. D., Crystal structure and powder data of davidite-type $La_2Ti_{10.27}Ga_{9.63}O_{38}$. *Powder Diffr.*, 1999, **14**(1), 36–41.
21. JCPDS Powder diffraction file, Card No: 42-0576.